

UDC 66.012.37

*Penza State University of Architecture and Construction**D. Sc. in Engineering, Prof. of Dept. of Applied Mathematics and Informatics**V. G. Kamburg**Russia, Penza, tel.: (8412)49-61-52; e-mail: kamburg@pguas.ru**Voronezh State Technological University**D. Sc. in Engineering, Prof., Head of Dept. of Industrial Energetics**V. V. Shitov**Russia, Voronezh, tel.: (4732)43-76-62; e-mail: rector@vorstu.ru*

V. G. Kamburg, V. V. Shitov

MATHEMATICAL MODELING AND INTENSIFICATION OF CONDENSATION GRAVITY FINE AIR FILTER OPERATION

Problem statement. A problem of mathematical modeling and intensification of operation of the flow thermal diffusion chamber of the condensation gravity filter as one of the most efficient air filter is solved.

Results and conclusions. This paper presents an example of the practical application of the model of heat and mass exchange in the thermodiffusion chamber as the main operating element of condensation gravity filter for high-performance air purification due to the generation of supersaturation fields with controlled properties. A criterion for quantitative assessment of purification efficiency in the form of breakthrough function is developed. The typical results of numerical modeling of the operation of the condensation gravity-type filter are presented for the most common case in practice. The possibility of intensification of the filter operation either at the stage of use or at the stage of design is shown based on the proposed approach, obtained models, and calculations.

Keywords: heat mass exchange, mathematical modeling, flow thermal diffusion chamber, controlled supersaturation fields, condensation gravity-type filter, air purification.

Introduction

One of the most perspective directions in the development of technology of fine purification of air or of other steam and gas flows from aerosols, detrimental compounds and pulverized particles is elaboration and application of condensation gravity-type filters (CGTF) with an operating body in the form of a flow thermal diffusion chamber (FTDC) [1—4].

These devices with a special supersaturation fields controlled by temperature, concentration and flow modes allow to change polluted substances from gaseous state to liquid state without classifying the particles according to their size. They are easily regenerated by water or by any other corresponding solution. Direct measurements of supersaturation fields are not easily obtained, their state is thus assessed by methods of physical mathematical modelling. The authors of papers [5—6] managed to study the most interesting from the practical viewpoint but most complicated from the viewpoint of modelling system solution (1)—(3) operation modes of FTDC with values of thermal and diffusion Pe Péclet coefficients close to 1. However, practical application of the results has not been up to now sufficiently examined.

The present paper offers a solution to mathematical modelling and intensification of FTDC operation process as a part of CGTF as a high-efficiency filter.

1. Theoretical description of the process of particle collection in CGTF

Let us study the general view of CGTF (Fig. 1) which is a device for fine air purification from aerosol particles with low concentration (up to 10.000 per cm^3) by steam condensation on a particle surface in a supersaturation fields produced and subsequent deposition of a suspended particle onto a lower wall of FTDC in a gravitational field.

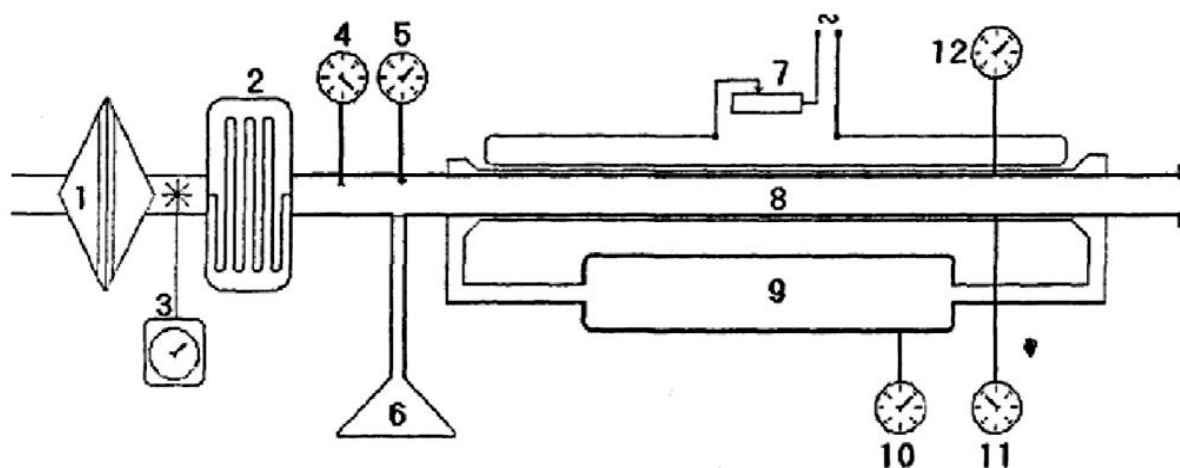


Fig. 1. Condensation gravity-type filter scheme:

- 1 is a coarse filter; 2 is a filter cleaning up to $\leq 10^{-2}$ mole per liter in impurities;
- 3 is a ventilation system with speed and flow temperature regulators; 4 is a flow speed regulator;
- 5 is a flow temperature regulator; 6 is a sediment collection container;
- 7 is a heat system for a hot plate with a regulator; 8 is a parallel-plate duct (FTDC);
- 9 is a surface-moisturizing system of; 10 is a water-expense regulator;
- 11 is a cold surface temperature regulator; 12 is a hot surface temperature regulator

FTDC is modelled by [1—6] in a form of a flat parallel-plate duct whose moisturized walls have temperatures T_1 and T_2 (Fig. 2).

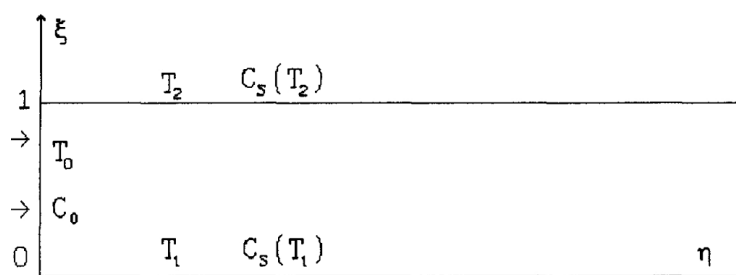


Fig. 2. Parallel-plate duct scheme:

$C_s(T_1)$ and $C_s(T_2)$ — saturated steam concentrations at temperatures T_1 and T_2 of corresponding FTDC walls

The steam concentration near the walls is considered saturated. The duct d height is much smaller than its length l and width w . Steam-gas mixture arrives at a duct entrance at an average motion speed $\langle V \rangle$, temperature T_0 and steam concentration C_0 . The position of a point within FTDC are given by coordinates $0 \leq x \leq d$, $0 \leq y \leq l$, while for dimensionless coordinates

$$\xi = x/d, \quad \eta = y/l, \quad (1)$$

$$0 \leq \xi \leq 1, \quad 0 \leq \eta \leq 1.$$

Distribution of saturation fields of temperature and steam concentration within FTDC is described by the following equation system whose numerical calculation algorithms and calculation examples are given in [5]—[6]:

$$\begin{aligned} 6Pe(\xi - \xi^2) \frac{\partial T(\xi, \eta)}{\partial \eta} &= \frac{\partial^2 T(\xi, \eta)}{\partial \xi^2} + \frac{\partial^2 T(\xi, \eta)}{\partial \eta^2}, \\ 6\overline{Pe}(\xi - \xi^2) \frac{\partial C(\xi, \eta)}{\partial \eta} &= \frac{\partial^2 C(\xi, \eta)}{\partial \xi^2} + \frac{\partial^2 C(\xi, \eta)}{\partial \eta^2}, \end{aligned} \quad (2)$$

where

$$Pe = \frac{\langle V \rangle d}{a_l}, \quad \overline{Pe} = \frac{\langle V \rangle d}{D_{12}}$$

are thermal and diffusion Péclet coefficients; a_l is a mixture thermal diffusivity coefficient; D_{12} is a gas steam diffusion coefficient.

Boundary conditions are:

$$\begin{aligned}
 T(\xi, \eta)|_{\eta \leq 0} &= T, \quad T(0, \eta) = T_1, \quad T(1, \eta) = T_2, \\
 T(\xi, l) &= T_1 + (T_2 - T_1)\xi = T_L, \\
 C(\xi, \eta)|_{\eta \leq 0} &= C_0, \\
 C(0, \eta) &= C_s(T_1) = C_1, \\
 C(1, \eta) &= C_s(T_2) = C_2, \\
 C(\xi, L) &= C_1 + (C_2 - C_1)\xi = C_L.
 \end{aligned} \tag{3}$$

The task of a path of different particles is solved for a horizontal parallel-plate duct (Fig. 3) with the following assumptions:

1) at a duct entrance and through its whole length gas flow is considered laminar, while speed distribution is described by the following formula (see [4, 7]):

$$v_z(x) = v_0 \left[\frac{4x}{d} - \left(\frac{2x}{d} \right)^2 \right]; \tag{4}$$

- 2) at a duct entrance aerosol particle concentration is stable along the whole section;
- 3) the particles do not interact, i. e. each particle moves independently from the others and their paths do not cross, which is a dilute solution condition ($\leq 10^{-2}$ mole per liter in an impurity);
- 4) a case of big aerosol particles with the size up to 25 mkm with low concentration whose speed is equal to one of moving gas;
- 5) the gravitational force affects the particle motion.

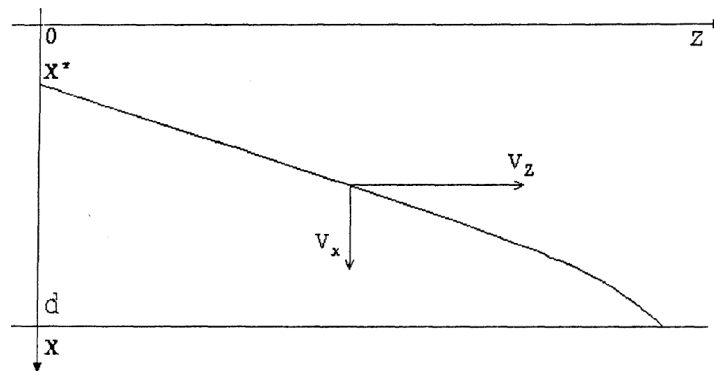


Fig. 3. A particle motion path in a FTDC parallel-plate duct

Considering a particle motion semi-uniform, we get the following particle motion path in a flat parallel-plate duct [7]:

$$\frac{dx}{dt} = v_x(t); \quad \frac{dz}{dt} = v_z[x(t)] \quad (5)$$

Under initial conditions

$$t_0 = 0; \quad x_0 = x^*; \quad z_0 = 0. \quad (6)$$

With the assumptions made, the expressions for vertical and horizontal speed components can take the following form

$$\begin{aligned} v_x(t) &= k_1(k[x(t)] \cdot t + R_0^2), \\ v_z[x(t)] &= v_0 \left[\frac{4x(t)}{d} - \left(\frac{2x(t)}{d} \right)^2 \right], \end{aligned} \quad (7)$$

$$k_1 = \frac{2\rho_i g}{9\mu_1}, \quad k(x) = \frac{\frac{D_{12}\mu_1 p_{l\infty}}{RT_{l\infty}\rho_i} \delta(x)}{1 + \left(\frac{\mu_1 L}{R} \right)^2 \frac{D_{12}p_{l\infty}}{\lambda_l(T_{l\infty})^3} C_{1s}(T_{l\infty})}, \quad (8)$$

where ρ_i is a drop density; $p_{l\infty}$ is a pressure at a long distance from a drop; R is the universal gas constant; $T_{l\infty}$ is a temperature at a long distance from a drop; L is a specific heat of evaporation; λ_l is a gas thermal conductivity coefficient; μ_1 is a steam molecular mass; $\delta(x, z)$ is a steam saturation at a specified duct point:

$$\delta(x, z) = \frac{C(x, z)}{C_s[T(x, z)]} - 1,$$

where $C(x, z)$ is a steam concentration at a specified point, $C_s[T(x, z)]$ is a saturated steam concentration at a specified point whose temperature relationship can be calculated by the known Clausius-Clapeyron formula:

$$C_s[T(x, z)] = \exp[A_0 - B_0 / T(x, z)],$$

where A_0 and B_0 are constants depending on a substance's physical properties.

With the assumptions made, equations for calculation of particle condensational growth take the following form

$$R(x, t) = \sqrt{R_0^2 + 2C_{1s}(T_{l\infty})k(x)t}. \quad (9)$$

2. Numerical calculation algorithm

Let us introduce the following designations:

$$x_i = x(t_i), \quad \Delta t = t_{i+1} - t_i. \quad (10)$$

Using simple numerical methods for the solution of the task (5)—(6), we can arrive at the following calculation scheme:

$$\begin{aligned} z_{i+1} &= v_0 \left[\frac{4x_i}{d} - \left(\frac{2x_i}{d} \right)^2 \right] \Delta t + z_i, \\ x_{i+1} &= k_1 \left[k(x_i)t_i + R_0^2 \right] \Delta t + x_i, \end{aligned} \quad (11)$$

$$x_0 = x^*, \quad z_0 = 0. \quad (12)$$

The calculations according to the scheme (11)—(12) are conducted till one of the following conditions is observed:

- 1) $x_i = d$ — a particle fell onto the lower wall of the duct;
- 2) $z_i > l$ — a particle flew out of the duct.

In practice, in filtration tasks these two cases describe the filter retrieving particles and breakthroughs, thus the correlation of these cases is a filter efficiency measurement. In order to conduct a quantitative assessment of this efficiency, we need to consider breakthrough coefficient.

Let us introduce a breakthrough function as a quantitative assessment of a filter efficiency in the form of a correlation of particles at the duct entrance and exit:

$$\begin{aligned} K &= \frac{N}{N_0}, \\ N_0|_{z=0} &= l \int_0^d n_0 v(x) dx, \quad N|_{z=l} = l \int_0^d n(x) v(x) dx, \end{aligned} \quad (13)$$

where N_0 is a particle flow at the duct entrance; N is a particle flow at the duct exit.

Taking into account the assumptions previously made, breakthrough coefficient can be calculated with the help of the limit path method.

According to assumption 3, paths of the particles do not cross, there is thus an initial coordinate x^* where all the particles with initial coordinates $x > x^*$ reach the lower wall and settle on it, while all the particles with initial coordinates $x < x^*$ will fly out of a duct. Thus, we get

$$N(z) = b \int_0^d n(x) v_z(x) dx = n_0 b \int_0^{x^*} v_z(x) dx \Big|_{z=0}. \quad (14)$$

Breakthrough coefficient therefore takes the following form:

$$K(z) = \frac{\int_0^{x^*} v_z(x) dx}{\int_0^d v_z(x) dx} = \frac{3}{2} \left[2 \left(\frac{x^*}{d} \right)^2 - \frac{4}{3} \left(\frac{x^*}{d} \right)^3 \right]. \quad (15)$$

However, the view of the function (4) and numerical experiments results indicate that there is such a coordinate $0 \leq x^{**} \leq x^*$ where all the particles with initial coordinates $x < x^{**}$ will fall onto the lower wall earlier than particles with initial coordinates $x^{**} < x < x^*$. This effect is explained by the fact that particles reach the maximum speed in the duct centre, while speed gradually recedes as they come nearer to the wall. Hence, the correlation of vertical and horizontal particle speed components that move in the vicinity to the walls turns out bigger than that of particles moving in the duct center, thus making them reach the lower wall faster. The following form of breakthrough coefficient is therefore more precise:

$$K(z) = \frac{\int_{x^{**}}^{x^*} v_z(x) dx}{\int_0^d v_z(x) dx} = \frac{4}{d} \left[\frac{(x^*)^2 - (x^{**})^2}{2} - \frac{(x^*)^3 - (x^{**})^3}{3d} \right]. \quad (16)$$

Formula (15) is a specified case of formula (16) when $x^{**} = 0$. It should be noted that particles paths do not cross provided their initial coordinates are $x > x^{**}$.

Writing breakthrough coefficient as a function from z allows to calculate this coefficient for each duct section as well as to consider the task of duct length optimization, etc.

3. Calculation examples and modelling results analysis

In Fig. 4 there are characteristic calculation results of a particle motion path with different working values of the specified parameters in the given coordinates ξ and η .

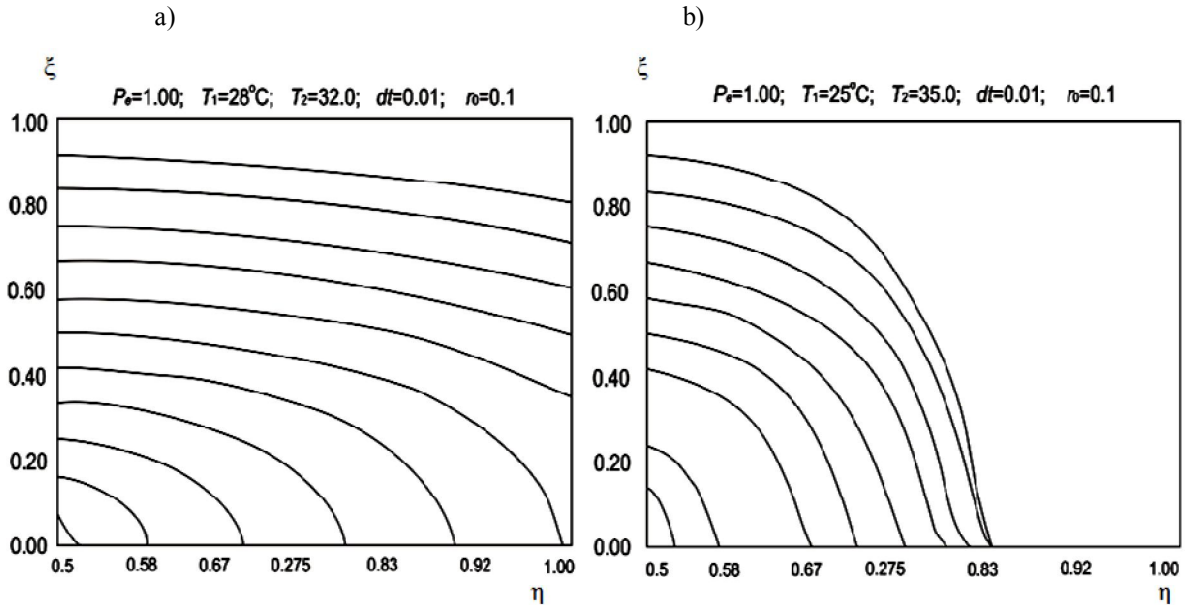


Fig. 4. Motion path $Z(x)$

In the above examples, there is a description of relations between motion paths and FTDC particles growth dynamics from the initial particle radius and saturation field. Motion paths are shown as functions whose value is coordinate z of a particle depending on a current coordinate x with various initial coordinates x (with a step $0.1 d$). Axis OX is thus selected for visual purposes so that the upper and lower walls have coordinates 0 and— 1 respectively (this should be taken into account during breakthrough coefficient calculations). A particle growth is shown as a function whose value is a particle radius, mkm , depending on a current coordinate z . Coefficient P_e is equal to 1.

At the first stage (see Fig. 2—4) we studied the saturation field effect with the initial particle radius $R_0=0.1 \text{ mkm}$. We also observed particles' paths and growth in a saturation field that appeared with temperature gradients 4, 10 and 20 degrees respectively. It was found that particles did not manage to grow with small temperature gradients and consequently most of them flew out the duct (see Fig. 2).

However, if a gradient increases, breakthrough coefficient K_{np} rapidly decreases (see Fig. 4): so, if $z=2$:

$$1) dT = 4: \quad x^* = 0.7, \quad x^{**} = 0.0, \quad K_{np} = 0.523;$$

$$2) dT = 10: \quad x^* = 0.4, \quad x^{**} = 0.0, \quad K_{np} = 0.235;$$

$$3) dT = 20: \quad x^* = 0.0, \quad x^{**} = 0.0, \quad K_{np} = 0.000.$$

In the third case $K_{np}=0$ starting from $z=1.2$; thus, there is a possibility of temperature mode optimization so that $K_{np}=0$ for coordinate z is not smaller than the specified one. Hence, the approach suggested, the algorithm elaborated and program package enable us to solve the task of a temperature gradient minimization for 100 % deposition depending on a duct length in condensation gravity-type filters.

At the second stage a similar case was examined, but initial particles' radii were 2 mkm. It was obtained that if $z=1.1$:

$$R_0 = 1: \quad x^* = 0.1, \quad x^{**} = 0.3, \quad K_{np} = 0.125.$$

In conclusion of these modelling numerical studies, we should note that a number of particles captured by FTDC can be characterized by a flow which arrives at a duct in a range of initial coordinates from 0 to x^{**} and from x^* to d and its quantitative assessment can be conducted using formula (16): $x^{**} \rightarrow 0$ as an initial radius increases and saturation field value decreases; $x^* \rightarrow 0$ as the saturation fields values or a particle initial radius increase while saturation field effect turns out much stronger; $x^{**} \rightarrow x^*$ as the saturation field values increase or a particle initial radius decreases; a particle growth in a duct is not largely dependent on its initial radius.

Conclusions

The characteristic resulting data on FTDC operation intensification dynamics for particle retrieval by the method suggested shows that a temperature gradient is one of the parameters of FTDC operation intensification as a basic operating element of a high-efficiency filter.

Based on these models, numerical research and necessary experiments in each case (duct geometry, flow operating environment, particles' size, their concentration, etc.), we can solve the task of CGTF capturing both individual particles and a flow as whole as well.

The set-up is turned into operation by specifying a hot surface temperature depending on the flow speed, its temperature, a cold wall temperature, a duct length. Limit paths and breakthrough coefficients are calculated on the basis of these parameters. A hot surface temperature is specified so that breakthrough coefficient is equal to 0.

Thus, we presented a method allowing to solve the task of CGTF operation process intensification for steam and gas flows with known geometrical and hydrodynamic FTDC parameters as well as with properties of aerosol particles retrieved. This method also helps to optimize these parameters in the process of CGTF construction and to choose its operation modes for specific tasks of ventilation and air purification.

References

1. James W. Fitzgerald, *Non-Steady-State Supersaturations in Thermal Diffusion Chambers* (Obninsk, 1970) [in Russian].
2. Yu. I. Yalamov, M. N. Gaidukov and Ye. R. Schukin, "Theory of Thermal Diffusion Motion of Moderately Large Volatile Aerosol Particles," *Zhurnal fizicheskoy khimii*, No. 2, 505 (1975).
3. G. N. Lipatov, "Experimental Study of Thermal Diffusion of Large Volatile Aerosol Particles," *Fizika aerodispersnykh system*, No. 19, 19 (1979).
4. G. N. Lipatov and A. S. Skaptsov, "Experimental Study of the Filtration Ability of Thermal Diffusion Chamber with Controlled Element," *Inzhenerno-fizicheskiy zhurnal*, No. 1, 93 (1984).
5. V. G. Kamburg and N. V. Sheptalin, "Generalized Model for Supersaturation Field Calculation in the Channels of Different Configurations," in *Integral transformations for boundary-value problems*. (Kiev, 1996), p. 21—26.
6. V. G. Kamburg, et al. "The Study of the Regularities of Supersaturation Field Formation in Flow Thermal Diffusion Chambers with the Use of Mathematical Modeling," *Vestnik Tekhnologicheskogo Universiteta Podolya (Khmelnitsky)*, No. 4, 14 (2002).
7. Z. L. Shulimanova and Ye. R. Shchukin, "Thermophoretic Precipitation of Aerosol Particles from Laminar Gas Flow on Cooled Surface," *VINITI*, No. 2879.